Physics Letters A 378 (2014) 800–803

Contents lists available at ScienceDirect

Physics Letters A

www.elsevier.com/locate/pla

Geodesic mode instability driven by the electron current in tokamak plasmas

A.G. Elfimov [a,*], A.I. Smolyakov [b], R.M.O. Galvão [a]

[a] Institute of Physics, University of São Paulo, São Paulo, 05508-090, Brazil
[b] University of Saskatchewan, 116 Science Place, Saskatoon, S7N 5E2, Canada

ARTICLE INFO

Article history:
Received 28 August 2013
Received in revised form 6 November 2013
Accepted 13 January 2014
Available online 21 January 2014
Communicated by F. Porcelli

Keywords:
Tokamak
Geodesic Acoustic Modes
Kinetic theory
Instability
Landau damping

ABSTRACT

Effect of the parallel electron current on Geodesic Acoustic Modes (GAM) in a tokamak is analyzed by kinetic theory taking into the account the ion Landau damping and diamagnetic drifts. It is shown that the electron current modeled by shifted Maxwell distribution may overcome the phase velocity threshold and ion Landau damping thus resulting in the GAM instability when the parallel electron current velocity is larger than the effective parallel GAM phase velocity $Rq\omega$. The instability occurs due to its cross term of the current with the ion diamagnetic drift. Possible applications to tokamak experiments are discussed.

1. Introduction

Geodesic Acoustic Modes (GAM) driven by geodesic plasma compressibility in toroidal geometry [1] have actively been studied theoretically in recent years [1–8]. Oscillations in the geodesic frequency range have been experimentally detected under wide range of condition in various tokamaks, during ohmic, neutral beam (NB), or ion cyclotron resonance heating (ICR) [7–16]. It is expected that these modes will interact and affect stationary plasma rotation [18,19] as well as drift-wave turbulence and plasma transport as has been observed in experiments [16] and simulations [19]. In general, GAM eigen-modes are subdivided into relatively high frequency geodesic mode (GAM) with frequency $\omega_{\mathrm{GAM}}^2 \approx (7T_i/2 + 2T_e)/R_0^2 m_i$ and ion-sound mode $\omega_s^2 \approx T_e/q^2 R_0^2 m_i$ [3–8,20] where R_0 is major radius, q is safety parameter, $T_{e,i}$ electron and ion temperatures. The high frequency modes are often observed as mixed with Alfvén eigenmodes (AE) (known as Alfvén cascades or reversed shear modes, chirping AE, and beta induced modes [7–11]). In T-10 tokamak experiments [14], the oscillations exhibiting GAM features are observed across a substantial part of the minor plasma radius, thus the local frequency of the GAM ω_{GAM} and the ion sound mode ω_s may be close to each other at some radial locations.

It is well known that ion sound instability [21] may be driven by an electric current along magnetic field. Typically, the instability occurs only when the electron beam velocity is higher than the ion sound velocity ($v_0 > c_s$) and the electron temperature is much larger than the ion temperature ($T_e \geqslant 6T_i$). Typically, a high electron current velocity may appear during current rump-up state or/and during a counter NB injection in tokamaks [10,15,22].

Here, we investigate whether the parallel electron current can drive the GAM modes via coupling with the drift dynamics. We present the kinetic treatment of the GAM type modes by fully taking into account parallel electron and ion dynamics and the ion diamagnetic drifts. Drift effect on GAM type modes was studied before [2,3,7,8], but the electron current was not included. A general kinetic treatment of geodesic eigenmodes is rather difficult, but the procedure is simplified for the geodesic continuum (GC). We do not consider here the eigen-mode structure, we consider only the continuum modes, similarly to other papers [3,4,6,7,17].

2. Dispersion equation

We employ the quasi-toroidal set of coordinates (r, ϑ, ζ) in the large aspect ratio tokamak approximation [9] $R_0 \gg r$, where the circular surfaces ($R = R_0 + r\cos\vartheta$, $z = r\sin\vartheta$) are formed by the magnetic field with toroidal and poloidal components, $B_\zeta = B_0 R_0/R$, $B_\vartheta = rB_\zeta/qR_0$, and $B_\vartheta \ll B_\zeta$. The cylindrical coordinate system is used in the velocity space, where $\{v_\perp, \sigma, v_\parallel\}$ are, respectively, the perpendicular, angular, and parallel components with respect of the magnetic field. The standard approach of small Larmor

* Corresponding author at: Institute of Physics, University of São Paulo, São Paulo, 05508-090, Brazil. Tel.: +55 11 3091 6809.
E-mail address: elfimov@if.usp.br (A.G. Elfimov).

0375-9601/$ – see front matter
http://dx.doi.org/10.1016/j.physleta.2014.01.018

radius is assumed to obtain a drift kinetic equation [21,23] in the form

$$\frac{\partial f}{\partial\vartheta}-\frac{\mathrm{i}\Omega f}{w}=\frac{eF}{mw}\left[\frac{(w-v_0)E_3}{k_0v_T^2}+\frac{2+\eta(w^2+u^2-3)}{2k_0v_T\omega_c d_r}E_2-\frac{(2w^2+u^2)}{2v_T\omega_c k_0R}E_1\sin\vartheta\right]. \tag{1}$$

Here $\Omega=\omega/k_0v_{Ti}$ and $\omega_c=eB/mc$ are the normalized wave and cyclotron frequencies, E_i are components of wave field where the parallel field E_3 is potential part of electromagnetic field, $E_3=h_\theta E_2$, $h_\vartheta=B_\vartheta/B_0$ is magnetic field inclination, $k_0=h_\vartheta/r$ is the parallel wave vector, $v_{Te,i}=\sqrt{T_{e,i}/m_{e,i}}$ are thermal velocities, $\partial n_0/\partial r=-n_0/d_r$ is density gradient, $\eta_{e,i}=\partial\ln T_{e,i}/\partial\ln n_0$, $w=v_\parallel/v_T$ and $u=v_\perp/v_T$ are normalized space velocities. For the $N=0$ toroidal mode number $k_0=1/qR$. Maxwell distribution function F is assumed for ions and the electron distribution is Maxwell distribution shifted by the parallel current velocity V_0, $F_e=F(1+v_\parallel V_0/v_{Te}^2)$. We use the potential approximation for the electric fields neglecting the magnetic perturbation. Integrating Eq. (1) for electrons in the limit $\omega\ll v_{Te}/qR$ ($\Omega\ll v_{Te}/v_{Ti}$ in our notation) and $V_0/v_{Te}=\mu v_0\ll 1$, we obtain the equations for the electron density perturbations $\tilde{n}_e$

$$\begin{aligned}n_s&=\frac{e_in_0R_0q}{T_e}\times\left[\sqrt{\frac{\pi}{2}}\mu\big(v_0+t_e\rho(1-\eta_e/2)\big)E_s-\left(1+\mathrm{i}\sqrt{\frac{\pi}{2}}\mu\Omega\right)E_c\right],\\ n_c&=\frac{e_in_0R_0q}{T_e}\times\left[\sqrt{\frac{\pi}{2}}\mu\big(v_0+t_e\rho(1-\eta_e/2)\big)E_c+\left(1+\mathrm{i}\sqrt{\frac{\pi}{2}}\mu\Omega\right)E_s\right]\end{aligned} \tag{2}$$

where $\mu=v_{Ti}/v_{Te}$, $E_3=E_s\sin\vartheta+E_c\cos\vartheta$, $\tilde{n}_e=n_s\sin\vartheta+n_c\cos\vartheta$ and the contribution of small electron diamagnetic drift velocity was combined with the contribution from the parallel current: $w_0=v_0+t_e\rho(1-\eta_e/2)$, where $\rho=v_{Ti}/d_r\omega_{ci}h_p$ is the normalized drift parameter. Then, using the radial magnetic drift velocity, we get the radial component of the electron current

$$\begin{aligned}\tilde{j}_r^e&=e\frac{v_{Te}^3}{2}\int_0^\infty u\,du\oint d\vartheta\int_{-\infty}^{\infty}V_{re}f_e\,dw\\ &=\frac{e_i^2qn_0}{m\omega_{ci}}\times\left[\mathrm{i}\sqrt{\frac{\pi}{2}}\frac{\mu}{2}\left(w_0+t_e\frac{\rho}{2}(2+\eta_e)\right)E_s-\left(1+\mathrm{i}\mu\sqrt{\frac{\pi}{2}}\frac{\Omega}{2}\right)E_c\right]\end{aligned} \tag{3}$$

where $V_{re,i}=-(2w^2+u^2)v_{Te,i}^2\sin\vartheta/2R\omega_{ce,i}$, and $t_e=T_e/T_i$. Using $v_0=0$ in Eq. (1) for ions, we get the equations for the $\sin\theta$- and $\cos\theta$-components of the perturbed distribution function

$$\begin{aligned}f_s&=\frac{\mathrm{i}e_i\Omega qRFE_s}{T_i(\Omega^2-w^2)}\left(w+\rho+\eta\rho\frac{(w^2+u^2-3)}{2}\right)-\frac{e_iqRFE_c}{T_i(\Omega^2-w^2)}\left(w^2+w\rho+w\rho\eta\frac{(w^2+u^2-3)}{2}\right)\\ &\quad-\frac{\mathrm{i}e_i\Omega q(2w^2+u^2)FE_1}{2\omega_{ci}m_iv_{Ti}(\Omega^2-w^2)},\end{aligned} \tag{4a}$$

$$\begin{aligned}f_c&=\frac{e_iqRwFE_s}{T_i(\Omega^2-w^2)}\left(w+\rho+\rho\eta\frac{(w^2+u^2-3)}{2}\right)+\frac{\mathrm{i}e_i\Omega qRFE_c}{T_i(\Omega^2-w^2)}\left(w+\rho+\eta\rho\frac{(w^2+u^2-3)}{2}\right)\\ &\quad-\frac{e_iqw(2w^2+u^2)FE_1}{2\omega_{ci}m_iv_{Ti}(\Omega^2-w^2)}.\end{aligned} \tag{4b}$$

These expressions define the ion density perturbations as follows:

$$n_{ic}=-\frac{e_in_0R_0q}{2m_iv_{Ti}^2}\times\left[(2+\sqrt{2}\Omega Z)E_s+\mathrm{i}\left(\frac{\sqrt{2}}{2}(2+\Omega^2\eta-\eta)Z+\Omega\eta\right)\rho E_c\right], \tag{5a}$$

$$\begin{aligned}n_{is}=\frac{e_in_0R_0q}{2m_{i0}v_{Ti}^2}\Big\{&\frac{\mathrm{i}v_{Ti}}{R_0\omega_{ci}}\big(\sqrt{2}(\Omega^2+1)Z/2+\Omega\big)E_1+\big[(2+\sqrt{2}\Omega Z)E_c\\ &-\mathrm{i}\big(\sqrt{2}(2+\Omega^2\eta-\eta)Z/2+\Omega\eta\big)\rho E_s\big]\Big\}.\end{aligned} \tag{5b}$$

Using the quasi-neutrality condition with the electron density from Eq. (2), one finds the electric field components in the form

$$E_s=\mathrm{i}\frac{\{\sqrt{2\pi}\mathrm{i}\mu w_0-\lfloor\sqrt{2}(\Omega^2\eta+2-\eta)Z/2+\eta\Omega\rfloor t_e\rho\}}{2[1+t_e(1+\sqrt{2}\Omega Z/2)+\sqrt{2\pi}\mathrm{i}\mu\Omega/2]}E_c, \tag{6a}$$

$$E_c=-\mathrm{i}\frac{t_ev_{Ti}[\Omega+\sqrt{2}(1+\Omega^2)Z/2]}{R_0\omega_{ci}D}\times\left[1+t_e\left(1+\sqrt{2}\Omega\frac{Z}{2}\right)+\frac{\sqrt{2\pi}}{2}\mathrm{i}\mu\Omega\right]E_1 \tag{6b}$$

where

$$D=\left[(\sqrt{2}Z/2+1)t_e+\sqrt{2\pi}\mathrm{i}\mu\Omega/2+1\right]^2-\frac{1}{4}\{[\sqrt{2}((\Omega^2-1)\eta/2+1)Z+\Omega\eta]t_e\rho-\mathrm{i}\sqrt{2\pi}\mu w_0\}^2. \tag{7}$$

The ion radial geodesic current is found from the ion distribution function in Eqs. (4a), (4b)

$$\begin{aligned}j_{ri}=\frac{e_i^2n_0q}{4m_i\omega_c}\Big\{&\mathrm{i}\rho\big[\sqrt{2}(\eta\Omega^4+2\Omega^2+2+\eta)Z/2+\eta\Omega^3+\Omega(2+\eta)\big]E_s\\ &-\big[\sqrt{2}\Omega(\Omega^2+1)Z+2\Omega^2+4\big]E_c\\ &-\frac{\mathrm{i}v_{Ti}}{R_0\omega_c}\big[(\Omega^4+2\Omega^2+2)Z+2\Omega(\Omega^2+3)\big]E_1\Big\}.\end{aligned} \tag{8}$$

The final equation for the geodesic continuum, which is obtained from the quasi-neutrality condition $\tilde{j}_r^e+\tilde{j}_r^i+j_p=0$, where j_p is the ion radial polarization current $j_p=-\mathrm{i}\omega c^2E_1/4\pi c_A^2$, $c_A=B/\sqrt{4\pi n_im_i}$ has the form

$$\Omega^2/q^2=\Psi/D \tag{9}$$

where Ψ is given by the expression

$$\begin{aligned}\Psi=&-D\big[\sqrt{2}(\Omega^4/2+\Omega^2+1)Z+\Omega(\Omega^2+3)\big]\Omega/2\\ &+t_e\frac{\Omega}{2}\big[\sqrt{2}(\Omega^2+1)Z/2+\Omega\big]\\ &\times\Big\langle\Omega\big[1+(\sqrt{2}\Omega Z/2+1)t_e+\sqrt{2\pi}\mathrm{i}\mu\Omega/2\big]\\ &\times\big[\sqrt{2}(\Omega^2+1)Z/2+\Omega-\sqrt{2\pi}\mathrm{i}\mu/2\big]\end{aligned}$$

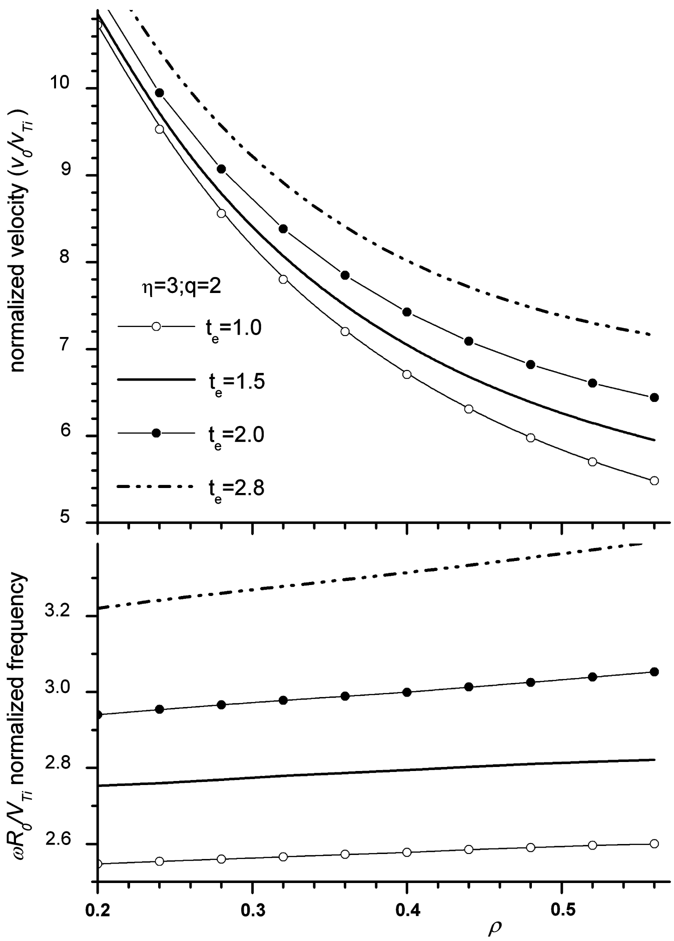

Fig. 1. Plot of the threshold velocity and the geodesic continuum frequency as a function of ρ for $\eta = 3$, $q = 2$, $t_e = 1.0, 1.5, 2$ and 2.8.

$$-\frac{1}{4}\left\{\left[\left((\Omega^4+1)\eta_i+2(\Omega^2+1)\right)\sqrt{2}\frac{Z}{2}+\Omega(\Omega^2+1)\eta_i\right.\right.$$
$$\left.+2\Omega\right]\rho+\sqrt{2\pi}\,\mathrm{i}\mu\left[w_0+t_e\frac{\rho}{2}(2+\eta_e)\right]\Bigg\}$$
$$\times\left\{\left[\sqrt{2}\left(2+(\Omega^2-1)\eta\right)Z/2+\Omega\eta\right]t_e\rho-\sqrt{2\pi}\,\mathrm{i}\mu w_0\right\}\Bigg\rangle. \qquad (10)$$

Here $Z=\int_{-\infty}^{\infty}dt\,\frac{\exp(-t^2)}{(t-x)}$ is the dispersion function, where $x=\Omega/\sqrt{2}$.

3. Discussion

The standard dispersion relation for the high frequency GAM may be found from Eq. (9) in the limit $\Omega \to \infty$ and assuming small imaginary part ($\gamma \ll \Omega_G$), which gives

$$\frac{\Omega_G^2}{q^2}=\left(\frac{\omega_G^2R_0^2}{v_{Ti}^2}\right)$$
$$\approx\left[\frac{7}{2}+2t_e+\frac{23+4t_e(4+t_e)}{q^2(7+4t_e)}+\frac{4\rho^2t_e^2(1+\eta_i+2t_e)}{q^2(7+4t_e)}\right]. \qquad (11)$$

The root corresponds to the GAM dispersion with the drift correction term similar to the expression from Eq. (5) of Ref. [8]. Assuming $\rho \ll w_0$, we find the imaginary part of the frequency γ

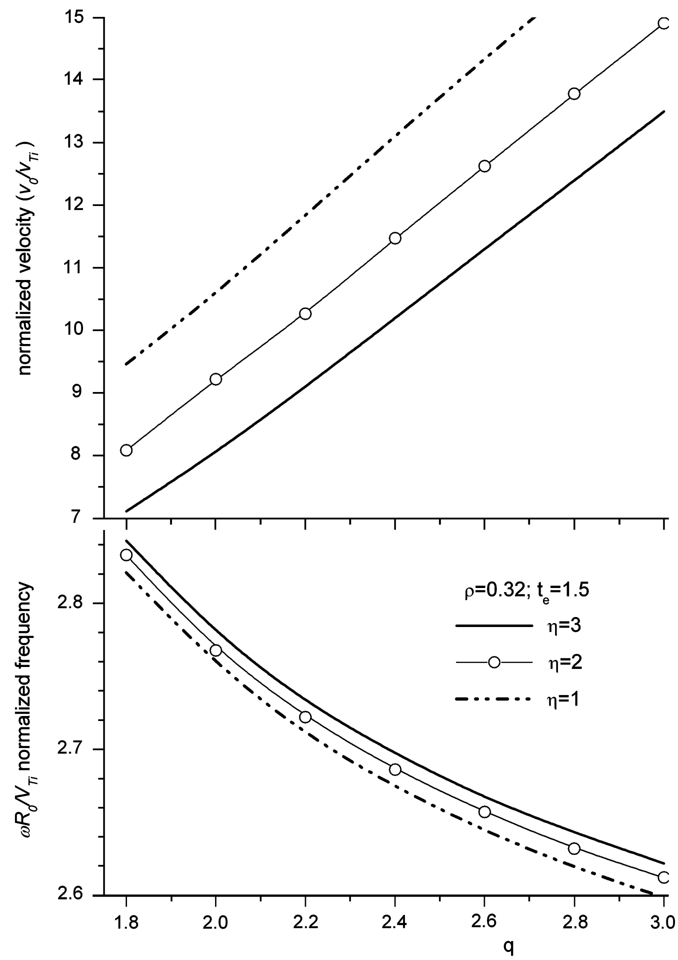

Fig. 2. Plot of the threshold velocity and the geodesic continuum frequencies as a function of q for $t_e = 1.5$, $\rho = 0.32$, and for different values of $\eta = 1, 2, 3$.

$$\gamma\approx\sqrt{\frac{\pi}{2}}\frac{v_{Ti}q}{2R_0}\left[\sqrt{t_e\frac{m_e}{m_i}}\left(\frac{\rho}{\Omega_G^2}(2+2\eta_i+3t_e)w_0-1-\frac{(8+4t_e)}{\Omega_G^2}\right)\right.$$
$$\left.-\frac{\Omega_G^2}{2}\left(\Omega_G^2+2+4t_e\right)\exp\left(-\frac{\Omega_G^2}{2}\right)\right]. \qquad (12)$$

For standard GAM at the continuum, the ion Landau damping [4] is exponentially small and the finite orbit effect (FOW) [23, 24] on the mode dissipation is ignored due to continuum approach $(k_r\rho_i q)^2 \ll 1$. In this case, the electron current may drive the GAM instability due to the cross-term of the current velocity and plasma density gradient, $\frac{V_0(1+\eta_i+3t_e/2)}{\omega_{ci}d_r} > \frac{\omega_G^2R_0^2}{2v_{Ti}^2}q^2$.

Asymptotic equations (11) and (12) are valid in the limit of large q. To accurately obtain the geodesic continuum mode and the threshold velocity for moderate values of q and ρ, we calculate the Ψ and D functions in Eq. (9) numerically. The results of calculation of the GAM frequency and the instability threshold are shown below as a function of the dimensionless parameters (t_e – electron/ion temperature ratio, q – safety factor, $\rho = v_{Ti}/d_r\omega_{ci}h_p$ normalized diamagnetic drift frequency, and $\eta = \eta_i = \eta_e$ the relative temperature gradient parameter). We note that threshold is defined by the formal condition $\gamma = 0$.

The threshold velocity decreases fast as an inverse function of the drift parameter as demonstrated in Fig. 1. The GAM frequency follows the GAM dispersion (12) and the proportional to the ρ-parameter. The ρ-parameter increases slowly with the electron temperature in the range ($1 \leqslant t_e \leqslant 2.8$).

Next, the dependence of the GAM frequency and the threshold as a function of q is shown in Fig. 2, for different values of the temperature gradient parameter.

Numerical calculations of the GAM continuum frequency shown in Fig. 2 mainly follow the analytical results in Eq. (7). The real frequency is weakly dependent of the η-parameter. The threshold velocity grows roughly linear with q-parameter and the dependence on η is more pronounced.

To clarify a physics reason of the instability, we appoint standing wave property ($M = 0, \pm 1$) of geodesic modes, when the inverse Landau drive for $k_\parallel = 1/qR$ is exactly compensated by the Landau damping for $k_\parallel = -1/qR$ and instability of the modes will be absent. For same reasons, only square of the drift frequency appears in the $N = 0$ GAM dispersion [3,7,8]. In our case of interplay (synergy effect) between the electron current and drift effect, the cross-terms like $k_\parallel V_0 \cdot M\omega_{drift} \sim \rho w_0$ may appear in the imaginary and real parts of the GAM dispersion, due to that we have the same sign for $M = \pm 1$ in these terms that is the origin the instability.

The presented results concerned with the GAM continuum. The eigenmode solutions are possible near the maximum or minimum of the continuum [6,11,25,26]. This condition may be realized in the case of reversed shear configurations observed in series experiments in tokamaks (e.g. in [9,10,15,22]). Finite Larmor radius effects [26] due to polarization current modification may determine the mode radial structure by the factor $(1 - (3/4)k_r^2 \rho_{Li}^2)$. Thus, the unstable geodesic eigenmode may have radial structure above continuum minimum $k_r^2 \rho_{Li}^2 \approx (1 - \omega_{G\,\min}^2/\omega^2)$. We note that similar dispersion may appear due to finite banana width effect [24].

Recently, during plasma current ramp up in JT-60 [22], the GAMs have been observed together with NB counter injection that forms reversed shear configuration. The modes are reported as energetic-particle geodesic modes (EGAMs) with the frequency approximately half of the core GAM frequency, but the modes do not appear during co-NB injection. That is something disagreement with existing EGAM theory [27] that also assumes the high energetic particle pressure of the order of the bulk pressure. A time-delay is necessary for the EGAM excitation to obtain the high pressure that does not observed in JT-60. Here, we present some alternative model of this effect. We suggest that this geodesic mode is the above-discussed unstable standard GAM with respective frequency driven by the electric current and localized at the q-minimum of the continuum that formed due to reversed shear configuration. The estimated velocity of the current at the $q = 4$ minimum $V_0 = 2rc_A^2/Rq\omega_{ci} \approx 4 \cdot 10^8$ cm/s $\gg \omega Rq$ is much higher then the GAM phase velocity that is necessary for instability and the time delay may be about few electron–ion collision time, which is necessary to transfer the ctr-NB energy and momentum to inverse the electron distribution. We also note that the FOW damping threshold [23] is very small for radial mode $k_r \leqslant \omega_{ci}/v_{Ti}q$ in comparison with electron one in Eq. (12).

Finally, we conclude that our analytical and numerical calculations show that the standard geodesic mode may be unstable when the current electron velocity of the Ohm's current is above the phase velocity $V_0 > \omega Rq$. The instability may be observed in the ramp up current phase in tokamaks with counter-NB injection at the position, where the inversed shear profile is formed. The instability is rather weak ($\gamma \propto \omega_{\mathrm{GAM}} v_{Ti}/v_{Te}$), but it may serve as some indicator for diagnostics of plasma parameters [10,11].

Acknowledgements

This work was supported by FAPESP (Research Foundation of the State of São Paulo), by CNPq (National Council of Scientific and Technological Development, Brazil), and NSERC Canada.

References

[1] N. Winsor, J.L. Jonson, J.M. Dowson, Phys. Fluids 11 (1968) 2448.
[2] A.B. Mikhajlovskii, Nucl. Fusion 13 (1973) 259.
[3] F. Zonca, L. Chen, R.A. Santoro, Plasma Phys. Control. Fusion 38 (1996) 2011.
[4] H. Sugama, T.-H. Watanabe, Phys. Plasmas 13 (2006) 012501.
[5] A.I. Smolyakov, C. Nguyen, X. Garbet, Nucl. Fusion 50 (2010) 054002.
[6] A.G. Elfimov, Phys. Plasmas 16 (2009) 034501.
[7] N.N. Gorelenkov, M.A. Van Zeeland, H.L. Berk, N.A. Crocker, D. Darrow, E. Fredrickson, G.-Y. Fu, W.W. Heidbrink, J. Menard, R. Nazikian, Phys. Plasmas 16 (2009) 056107.
[8] F. Zonca, L. Chen, Nucl. Fusion 49 (2009) 085009.
[9] W.W. Heidbrink, E. Ruskov, E.M. Carolipio, J. Fang, M.A. van Zeeland, R.A. James, Phys. Plasmas 54 (1999) 1147.
[10] H.L. Berk, C.J. Boswell, D. Borba, A.C.A. Figueiredo, T. Johnson, M.F.F. Nave, S.D. Pinches, S.E. Sharapov, Nucl. Fusion 46 (2006) S888.
[11] A.G. Elfimov, R.M.O. Galvão, S.E. Sharapov, Phys. Plasmas 17 (2010) 110705.
[12] A.V. Melnikov, V.A. Vershkov, L.G. Eliseev, S.A. Grashin, A.V. Gudozhnik, L.I. Krupnik, S.E. Lysenko, V.A. Mavrin, S.V. Perfilov, D.A. Shelukhin, S.V. Soldatov, M.V. Ufimtsev, A.O. Urazbaev, Czechoslov. J. Phys. 55 (2005) 349.
[13] G.D. Conway, B. Scott, J. Schirmer, M. Reich, A. Kendl, Plasma Phys. Control. Fusion 47 (2005) 1165.
[14] A.V. Melnikov, V.A. Vershkov, L.G. Eliseev, S.A. Grashin, A.V. Gudozhnik, L.I. Krupnik, S.E. Lysenko, V.A. Mavrin, S.V. Perfilov, D.A. Shelukhin, S.V. Soldatov, M.V. Ufimtsev, A.O. Urazbaev, G. Van Oost, L.G. Zimeleva, Plasma Phys. Control. Fusion 48 (2006) S87.
[15] R. Nazikian, G.Y. Fu, M.E. Austin, H.L. Berk, R.V. Budny, N.N. Gorelenkov, W.W. Heidbrink, C.T. Holcomb, G.J. Kramer, G.R. McKee, M.A. Makowski, W.M. Solomon, M. Shafer, E.J. Strait, M.A. Van Zeeland, Phys. Rev. Lett. 101 (2008) 185001.
[16] G.R. McKee, R.J. Fonck, M. Jakubowski, K.H. Burrell, K. Hallatschek, R.A. Moyer, D.L. Rudakov, W. Nevins, G.D. Porter, P. Schoch, X. Xu, Nucl. Fusion 49 (2009) 115016.
[17] A.G. Elfimov, R.M.O. Galvão, R.J.F Sgalla, Plasma Phys. Control. Fusion 53 (2012) 105003.
[18] A. Smolyakov, Elements of neoclassical theory and plasma rotation in a tokamak, in: Biennial Reviews of the Theory of Magnetized Plasmas, World Scientific, 2013.
[19] K. Hallatschek, D. Biskamp, Phys. Rev. Lett. 86 (2001) 1223.
[20] Z. Gao, K. Itoh, H. Sanuki, J.Q. Dong, Phys. Plasmas 13 (2006) 100702.
[21] R.J. Goldston, P.H. Rutherford, Introduction to Plasma Physics, Institute of Physics Pub., Bristol, 1995.
[22] G. Matsunaga, K. Kamiya, K. Shinohara, N. Miyato, A. Kojima, A. Bierwage, in: Proceedings of 39th EPS Conference & 16th Int. Congress on Plasma Phys., Stockholm/Sweden, July 2012, in: EPS Abstract Series, Stockholm/Sweden, 2012, P2.062.
[23] H. Sugama, T.-H. Watanabe, J. Plasma Phys. 74 (2007) 139–140.
[24] A.G. Elfimov, A.I. Smolyakov, A.V. Melnikov, R.M.O. Galvão, Phys. Plasmas 20 (2013) 052116.
[25] S.I. Itoh, K. Itoh, M. Sasaki, A. Fujisawa, T. Ido, Y. Nagashima, Plasma Phys. Control. Fusion 49 (2007) L7–10.
[26] Z. Qiu, F. Zonca, L. Chen, Plasma Phys. Control. Fusion 52 (2010) 095003.
[27] G.Y. Fu, Phys. Rev. Lett. 101 (2008) 185002.